Ultrafast Spectroscopy of Excitons in Semiconducting Carbon Nanotubes

C. X. Sheng[a], Z. V. Vardeny[a], A.B. Dalton[b] and R.H. Baughman[c]

[a] Department of Physics, University of Utah, Salt Lake City, Utah 84112

[b] Department of Physics and UniS Material Institute, University of Surrey, Guildford GU2 7XH U.K.

[c] NanoTech Institute, University of Texas at Dallas, Richardson, Texas 75083

Abstract

Ultrafast relaxation dynamics of photoexcitations in semiconducting single walled carbon nanotubes (*S*-NTs) were investigated using polarized pump-probe photomodulation (with 150 fs time resolution) and cw polarized photoluminescence (PL). Both annealed and unannealed NT films and D_2O solutions of isolated NTs were investigated. Various transient photoinduced bleaching (PB) and photoinduced absorption (PA) bands, which show photoinduced dichroism, were observed in the ultrafast photomodulation spectra of *all* NT forms. Taking into account the PB spectral shift observed for NTs in solution, the PA and PB bands are seen to decay together by following a power law in time of the form $(t)^{-\alpha}$, with α in the range of 0.7 to 1. The PL emission of *S*-NTs in D_2O solution shows a polarization degree that agrees with that of the transient photoinduced dichroism. We conclude that the primary photoexcitations in *S*-NTs are excitons that are confined along the NTs. From the average PL polarization degree and the transient polarization memory decay, we estimate the PL lifetime of isolated NTs in solution is of order 500ps. This relatively long PL lifetime is dominated by non-radiative decay processes, which when coupled with the tiny PL emission quantum efficiency indicates a very small radiative recombination rate, in good agreement with recent theories that include electron correlation.

Keywords: Photoluminescence, non-linear optical methods, carbon nanotubes, ultrafast dynamics

1. Introduction

Carbon nanotubes (NTs) have very interesting mechanical [1] and electronic [2,3] properties, which have stirred the interest of many research groups during the past decade. Recently developed methods for spatially separating single-walled carbon NTs (SWCNTs) have enabled such basic optical studies as polarized absorption [4,5] and Raman scattering [6,7] on films of unbundled NTs. Photoluminescence (PL) emission has been observed for semiconducting (*S-)* NTs suspended in D_2O solutions [8,9] and for single isolated NTs [7,10]. Recently electroluminescence of a single *S*-NT has been realized [11,12]. The PL emission measurements have refocused questions concerning the nature of the primary photoexcitations in *S*-NTs. In particular, the role of excitons in the optical spectra of *S*-NTs has been reinstated, since excitons are responsible for the measured PL [8-10]. Very good overlap was found between the measured bands in the optical absorption and those in the PL emission spectrum [13,14]. In addition, electron energy calculations of *S*-NTs in which electron-electron and electron-hole interactions have been explicitly included show a large exciton binding energy, in part because of the enhanced Coulomb interaction in these quasi-1D systems [15-23]. As a matter of fact, the results of the model calculations for excitons in NTs are similar to those of excitons in π-conjugated polymers, which also show large binding energies [24-26], indicating that excitons in quasi-1D systems may have common properties.

Recent experimental studies of the nonlinear optical properties and photoexcitations dynamics in SWCNTs have demonstrated ultrafast kinetics, and therefore potential optoelectronic applications were proposed. For example, femtosecond (fs) time-resolved photoemission measurements were done on annealed metallic NTs (*M*-NTs), which show that the excited electron lifetime decreases from 130 fs at 0.2 eV, to less than 20 fs at 1.5 eV above the Fermi energy [27]. Chen et al. [28] reported sub-picosecond relaxation kinetics of excited states in NT/π-conjugated-polymer composites at probe energy of 1.55 μm, which showed that NTs could be used in principle for ultrafast switching in optical

Ultrafast Phenomena in Semiconductors and Nanostructure Materials IX,
edited by Kong-Thon Tsen, Jin-Joo Song, Hongxing Jiang, Proc. of SPIE Vol. 5725
(SPIE, Bellingham, WA, 2005) · 0277-786X/05/$15 · doi: 10.1117/12.590801

communication technology. It has also been shown [29] that resonant excitation of *S*-NTs enhances the third order nonlinear optical coefficient $\chi^{(3)}$, which was found to be as high as 10^{-7} esu. Lauret *et al.* [30] discussed the recombination kinetics of photoexcitations in pump-probe measurements under resonant excitation conditions in *S*-NTs, which occurs on a 1 ps time scale. They observed photoinduced bleaching (PB) when pumping at or above the interband transitions, and photoinduced absorption (PA) when pumping at lower photon energies; which they attributed to the red shift of the global π-plasmon in the NTs. Our group [31] has recently reported transient photomodulation spectra of both *S*- and *M*-NTs using a low-repetition-rate, high-power ultrafast laser system that generated large photoexcitation densities of the order of $5x10^{19}/cm^3$. We found various PB and PA bands in *S*-NTs that are correlated with each other. From these findings, we concluded that the primary photoexcitations in *S*-NT are excitons rather than free carriers. In *M*-NTs, on the contrary we showed that the primary photoexcitations are hot carriers. Ostojic et al.[32] have recently reported the transient photoexcitation kinetics of *S*-NTs in D_2O solutions, and showed that the decay kinetics is dependent on the solution pH.

Here we report ultrafast time-resolved studies of photoexcitations dynamics of *S*-NTs in annealed and unannealed NT films, and isolated NTs in D_2O solution, using a high-repetition-rate low power laser system that generates a photoexcitation density of the order of $10^{16}/cm^3$. The low photoexcitation density enabled us to study the intrinsic photoexcitation dynamics without the complication of exciton-exciton and/or pump-photon/exciton interactions, which characterize high power laser systems. We used the polarized pump and probe technique, where the probe spans a variety of wavelengths in the mid infrared spectral range, using transient photomodulation (PM) spectroscopy with 150 fs time resolution.

We found that the transient PM spectra of all investigated nanotube samples contain both PA and PB bands that are similar, but not exactly the same, as those found in our previous work for annealed NTs [31]. When taking into account the transient spectral shift that we observed in the PB bands, we conclude that the decay dynamics of the various bands in the transient PM spectrum characterize a common type of primary photoexcitation. In addition, the PM bands show transient photoinduced dichroism, or polarization memory in *all* NT samples, where $(\Delta T/T)_{\parallel} \neq (\Delta T/T)_{\perp}$; here $\parallel$ and $\perp$ denote pump-probe polarization either parallel or perpendicular to each other, and $\Delta T/T$ is the fractional change in transmission, T. The prompt polarization memory, P(t) decays at various rates depending on the form of the investigated NT sample and the excitation photon energy. The fastest decay was measured for NTs in annealed films, whereas the slowest decay was found for isolated NTs in D_2O solution. We found that the polarization memory is consistent with confined photoexcitations, so that the primary photoexcitations in NTs cannot be delocalized free carriers, as previously assumed [28-30, 32]. We also measured PL emission for isolated NTs in D_2O solution, and found the same emission spectrum as the absorption and transient PB spectra; in addition, the PL is polarized. The PL polarization degree equals the transient photo-induced polarization memory that we measured at long times (of order of 1 ns). We therefore conclude that the primary photoexcitations in *S*-NTs are *excitons* rather than free carriers in continuum bands. From the tiny PL quantum efficiency, the polarization memory decay in the transient response, and the polarization degree of the PL emission, we estimate the radiative recombination time of isolated NTs in solution to be 3±2 μsec.

We also found that the photoinduced exciton dynamics depend on the NT form; however the various photoinduced PB and PA bands are basically the same in all three types of NT samples. The exciton dynamics is fastest for the annealed samples and slowest for NTs in D_2O solution. The different exciton dynamics and polarization memory decays for the annealed and unannealed NTs, as well as for the NTs in D_2O solution, show that impurities and/or defects in the NTs have a profound influence on the electronic relaxation processes.

2. Experimental

The single walled carbon NTs used for our studies were prepared using the HiPco process, and were supplied by CNI [11]. Typically, the raw material contains 85% wt. % nanotubes and 15 % iron catalyst nanoparticles. The NTs were dispersed in H_2O or D_2O using the surfactant lithium dodecyl sulfate. Specifically, 0.4 wt. % NTs were added to a 1.2 wt. % LDS aqueous solution. Sonication was then performed using a VWR Scientific Branson Sonifier 250 with the sample immersed in an ice water bath. Samples were sonicated 20 min at a power level of 30 W, yielding dark black mixtures. Films were prepared by successive dip coating of glass substrates into the H_2O solutions. When the NT film is put in a chamber filled with argon gas and heated to 600°C for 6 hours, the annealing process removes most of the LDS. Otherwise the unannealed film is used as grown in our optical set-up. From resonant Raman scattering measurements [31] we inferred

that our samples contained *M*-NTs as well as *S*-NT with an approximate ratio of 1:2, having a diameter distribution from 0.7 to 1.4 nm with a peak in the distribution at a diameter of ~1.0 nm.

Dispersions of predominantly isolated nanotubes in D_2O were prepared using a procedure based on the method developed by O'Connell et al.[8] The sonicated samples were first centrifuged in an Eppendorf 5417C centrifuge for 10 min. at 700 x g. The upper 75% of the supernatant was recovered using a small-bore pipette, avoiding sediment at the bottom, and transferred to a Beckman centrifuge tube for further centrifugation. Samples were then centrifuged for 2 hours at 100,000 x g in a Beckman TL-100 ultracentrifuge with the temperature controlled at 4°C. The upper 50% of the supernatant was then recovered using a small-bore pipette, again avoiding sediment at the bottom, and transferred to a clean tube. High-speed centrifugation sedimented the non-dispersed NTs as a pellet, yielding homogeneous gray dispersions.

For our ultrafast spectroscopy studies, we used the fs two-color pump-probe correlation technique with linearly polarized light beams for measuring the transient PM in the range between 0.55 and 1.05 eV. Our ultrafast laser system was a 100 fs Ti-sapphire oscillator operating at a repetition rate of about 80 MHz, which pumped an optical parametric oscillator (OPO) (Tsunami, Opal, Spectra-Physics) where both signal and idler beams were used as probe beams. The pump beam was extracted either from the fundamental at ~ 1.6 eV or from the signal beam at ~ 0.93 eV. To increase the signal/noise ratio, an acousto-optical modulator operating at 85 KHz was used to modulate the pump beam intensity. For measuring the transient response at time t with ~ 150 fs time resolution, the probe pulses were mechanically delayed with respect to the pump pulses using a translation stage; the time t = 0 was obtained by a cross-correlation between the pump and probe pulses in a nonlinear optical crystal. Typically the pump intensity was kept lower than 5 $\mu J/cm^2$ per pulse, which corresponds to ~ $10^{16}/cm^3$ initial photoexcitation density per pulse in the NT films. This density corresponds to less than a single photoexcitation per NT for the NTs in D_2O solution. The transient PM signal, $\Delta T/T(t)$, is the fractional change in transmission, T; which is negative for PA and positive for PB. The pump beam passed though a polarization rotator that changed its polarization to be 45° to that of the probe beam. An optical polarizer was used on the transmitted probe beam to analyze the changes of transmission, ΔT for both parallel $\Delta T_{\|}$, and perpendicular $\Delta T_{\perp}$, polarizations [22]. The transient polarization memory, $P(t) = (\Delta T_{\|} - \Delta T_{\perp})/(\Delta T_{\|} + \Delta T_{\perp})$, was then calculated to study its decay. The pump and probe beams were carefully adjusted to get complete spatial overlap on the film, which was kept under dynamic vacuum. In addition the pump/probe beam-walk with the translation stage was carefully monitored and the transient response was adjusted by the beam-walk measured response.

For the cw polarized PL emission study, we used the fundamental of the Ti-sapphire laser system at 1.6 eV operating at full power (1.5 Watt) to excite the isolated *S*-NT in the D_2O solution. The PL emission was collected by a lens with large F-number, and spectrally and spatially filtered to eliminate the relatively strong excitation laser intensity. A polarizer was used to select the PL emission either parallel or perpendicular to the polarization of the pump beam, and a polarization scrambler in front of the monochromator was used to detect the two PL components through the spectrometer. The collected PL emission was then directed onto the exit slit of a ¼ meter monochromator with 1 nm resolution; a nitrogen cooled germanium photodiode was used for the light detection in the near and mid infrared spectral ranges. The PL spectrum was corrected for the background system response obtained when the NT solution was replaced by a solution from the same solvent that did not contain NTs.

3. Results and Discussion

Typical optical absorption spectra, $\alpha(\omega)$, for the annealed and unannealed NT films and isolated NTs in solution are shown in Fig.1. Absorption bands A, B, D in Fig. 1(a) for the NT films were previously assigned to the various inhomogeneously broadened interband optical transitions of the *S*-NTs in the sample. The absorption bands in this model are due to dipole allowed symmetrical transitions from various valence subbands to their respective conduction subbands having the same index, m; namely m = ±1, ±2, and ±3, respectively. Band C, on the contrary is the first interband transition (m = ±1) of the *M*-NTs in the sample [27, 30]. The absorption features related to the quasi-1D character of the NTs are more pronounced in the annealed sample, in agreement with the results of Itkis *et al.* [35], suggesting that the annealing process purifies the NTs. This can be understood since the annealing process removes substituent groups that result from oxidation during nanotube purification. The background absorption in Fig. 1(a) was assigned to the absorption tail of the π-plasmon resonance (that peaks at about 5 eV), which does not change much as a result of annealing the film samples [36].

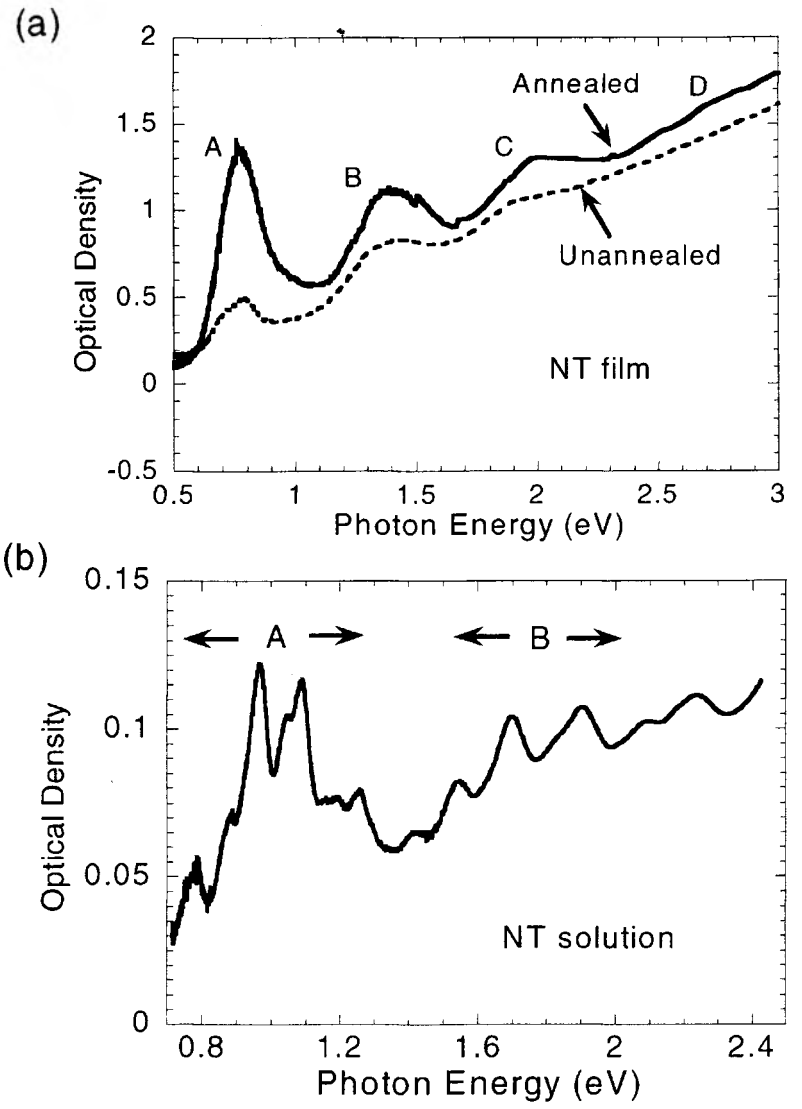

Figure 1: Absorption spectra, $\alpha(\omega)$, of SWCNT of different forms. (a) Annealed (solid line) and unannealed (dashed line) NTs films, and (b) NTs in D_2O solution. The bands A, B and D are due to *S*-NT transitions; band C is due to *M*-NT transition.

In contrast to the SWCNT films, the absorption spectrum $\alpha(\omega)$ of NTs in D_2O solution (Fig. 1(b)) contains a number of isolated sub-bands that belong to band A, B, and C, respectively. This shows that the inhomogeneity of the NTs in D_2O solution is smaller than for the films; the NTs are probably unbundled or bundled in more specific groups of NTs having the same diameter compared to those in films, and show less disorder. It is also noteworthy that the absorption background in $\alpha(\omega)$ is suppressed in the D_2O solution. This is surprising and calls for revisiting the explanation given for the absorption tail of NTs in NT films[36]. When comparing Figs. 1(a) and 1(b), we note that peak A in films is at lower photon energy than the individual peaks in group A in solution; also the bands marked B in the solution may in fact also

contain peaks from band C in the films. Since the only difference between the NTs in films and solution is the NT isolated in the latter, the decrease in resonant energy shows either that the Van-der Waals interaction in films is of the order of 0.2 eV, or that the exciton binding energy in NTs depends on the dielectric constant of the surrounding [22]. The different resonant energy of band A in films and solution presumably does not have a profound influence over the transient photoexcitation dynamics that is the focus of this work, since the pump photon energy is above band A in both cases. Also we expect that traps dominate the exciton dynamics [31]; in this case the exciton binding energy has little influence over the escape probability from the traps [37].

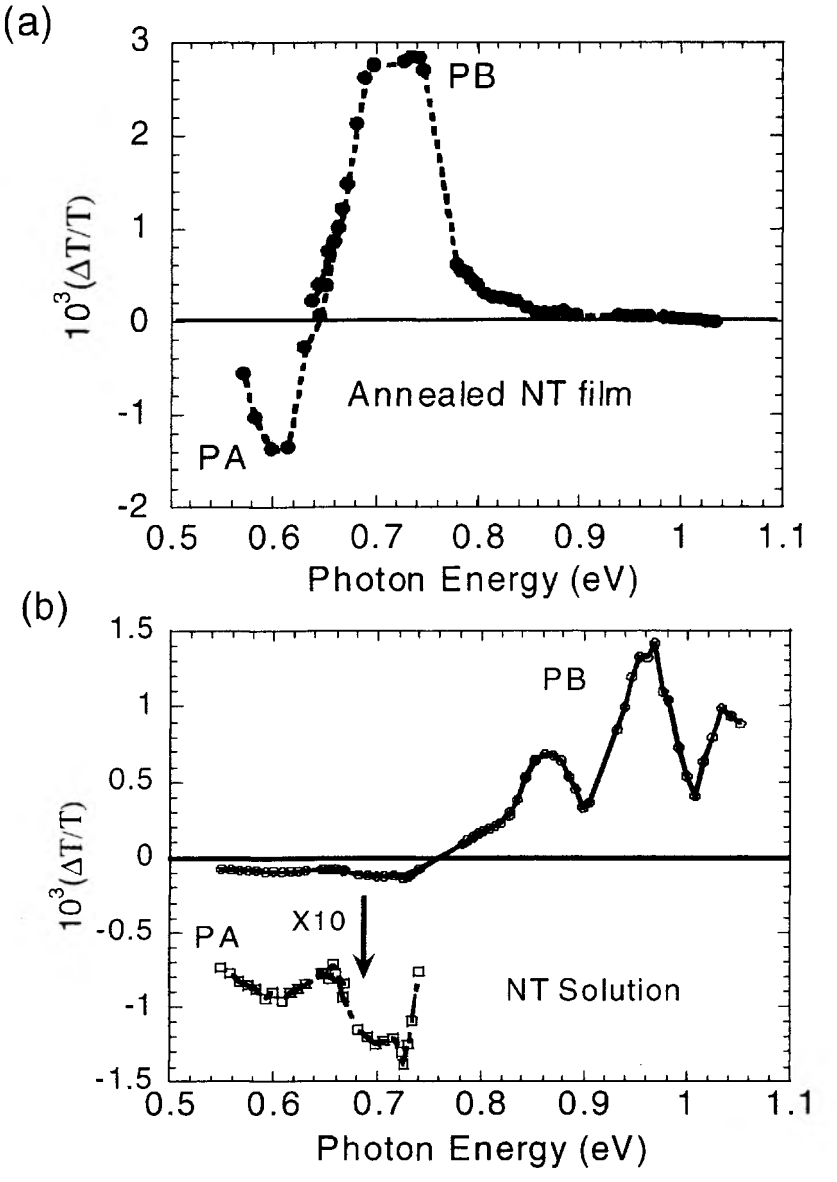

Figure 2: Transient PM spectra measured at t = 0 for an annealed SWCNT film (a) and NTs in D_2O solution (b). Various PA and PB bands are assigned.

In Fig. 2 we show the transient PM spectra of *S*-NTs in the annealed film and D_2O solution in the mid infrared spectral range and at t = 0. The PM spectra were photogenerated with pump photon energy at 1.6 eV, which preferentially excites *S*-NT; excitations in *M*-NT are mainly photogenerated at 1.9 eV and higher [27, 30-31]. This has been also derived from resonant Raman scattering studies [3, 38-39]. The PM spectra contain both PB and PA bands and thus cannot originate from a shift in the global plasmon [30]; these are therefore photoinduced bands associated with specific optical transitions of the primary photoexcitations in *S*-NTs [31]. The PB bands in both films and solution are within the spectral range of band A in the respective absorption spectra (Fig. 1), and are thus due to either k-space state filling or Q-space filling, depending on whether carriers or excitons are photogenerated in *S*-NTs at t = 0. From their similar dynamics and polarization memory decay it was previously concluded [31] that the transient PB and PA bands in the mid-ir spectral range are correlated, and thus the PA bands is due to optical transitions of photoexcitations that occupy electronic states associated with band A in the absorption spectrum. Note that the transient PB band is more structured for NTs in solution than for NTs in films, which agrees with the observation of more structure in the absorption subbands of the $\alpha(\omega)$ spectrum for NTs in solution.

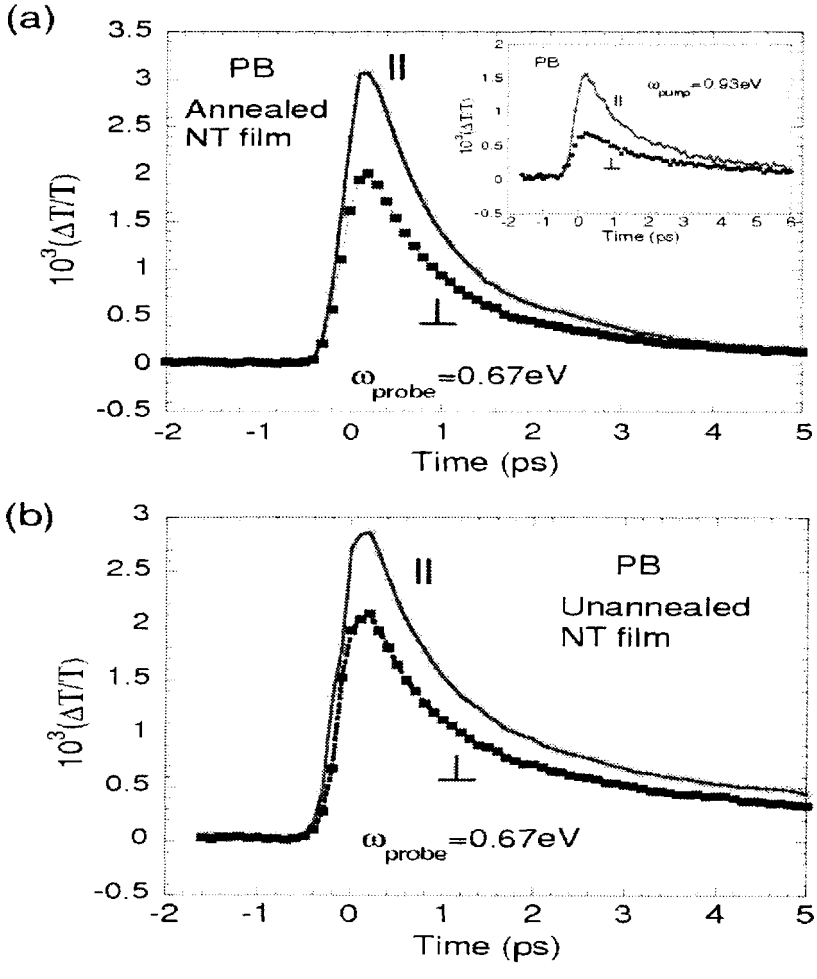

Figure 3: Transient polarized PB response at 0.67 eV for SWCNT of different forms: both $\Delta T_{\parallel}$ and $\Delta T_{\perp}$ components are shown. (a) Annealed film excited with two different pump photon energies (see inset); (b) unannealed film.

The exciton dynamics in the unannealed and annealed NT films were studied by measuring the transient polarized response for specific wavelengths within the PB bands, as shown in Fig. 3. The transient PB decays faster in the annealed film compared with that in the unannealed film. More specifically, the PB decay time constant, τ (defined as the time to reach N(0)/3, where N(0) is the initial exciton density) is about 1 ps in the annealed film (Fig. 3(a)), compared with $\tau = 2$ ps for the unannealed film (Fig. 3(b)). The slower dynamics in the unannealed film is probably due to excess disorder that may give rise to shallow traps that slow down the exciton recombination kinetics in this film [41-43]. Annealing heals defects and removes surfactants, which decrease the states due to shallow traps in the electronic density of states [42]. When excited within band A at 0.93 eV (Fig. 3(a) inset), then the decay rate of the PA in the annealed film is slower, with $\tau \approx 1.5$ ps. This shows that the exciton dynamics is slower when excited resonantly, in agreement with recent measurements of Ostojic *et al.* [32].

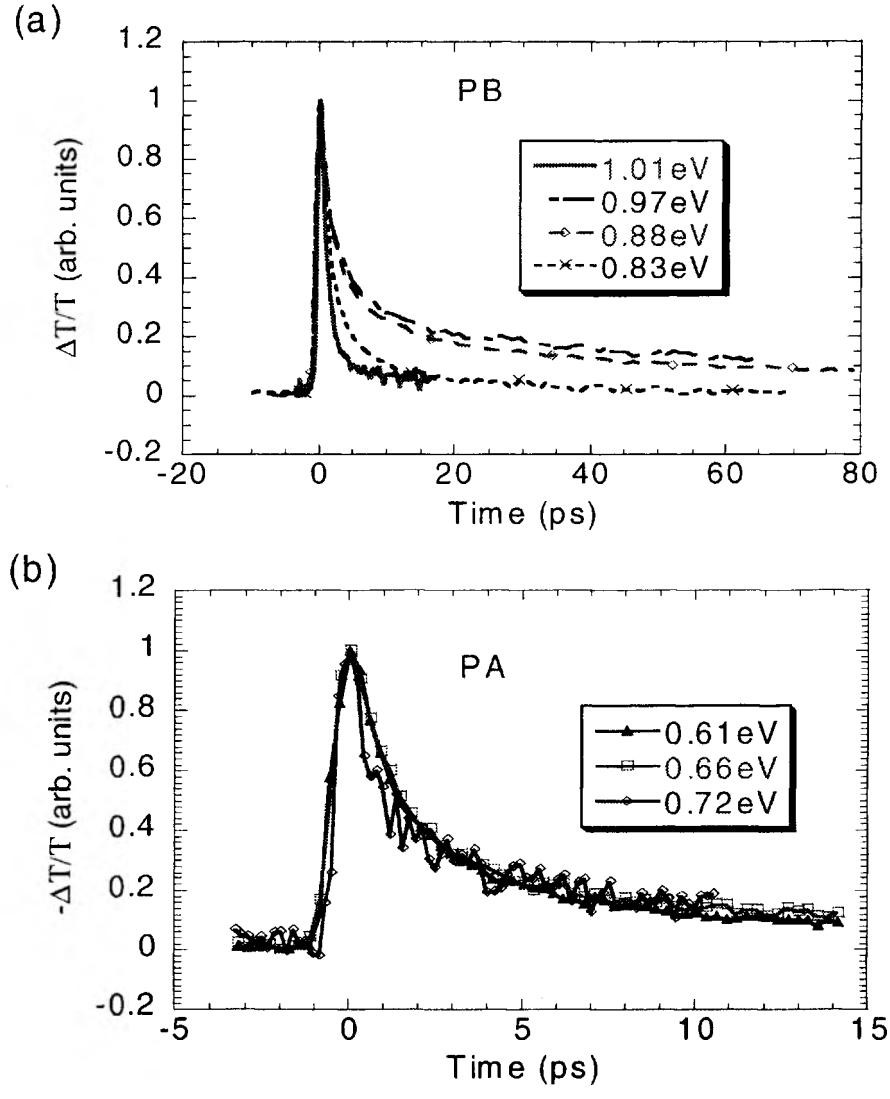

Figure 4: Transient polarized PM response of NTs in D_2O solution excited at 1.6 eV and probed at various photon energies within the PB bands (a), and PA bands (b).

The decay of PB for NTs in D_2O solution is much slower compared to that for NT films (Fig. 4). In addition, it seems that the decay dynamics changes across the PB spectrum. At ω_{probe} = 1.01 eV, which is close to a dip in the PB and $\alpha(\omega)$ spectra, we obtained for the PB decay $\tau \approx 3$ ps (Fig. 4(a)); whereas at ω_{probe} = 0.97 eV, which is at a maximum in both PB and $\alpha(\omega)$ spectra, we obtained $\tau \approx 8$ ps (Fig. 4(a)), with a tail towards longer times. This indicates that NTs in solution are also subject to disorder and inhomogeneity, which might be due to the added surfactants used for obtaining NT dispersion in solution. This disorder results in states in the gap, or shallow traps that may decrease the exciton recombination rate [41-43]. The different decay dynamics across the PB spectrum can be more clearly seen in Fig. 5(a), where the transient PB spectrum is depicted. It is seen that the PB spectrum blue-shifts with time for each absorption sub-band in $\alpha(\omega)$. Fig. 5(a) inset summarizes the shift of the PB maximum photon-energy in the first peak at 0.87 eV vs. time. It is seen that the PB

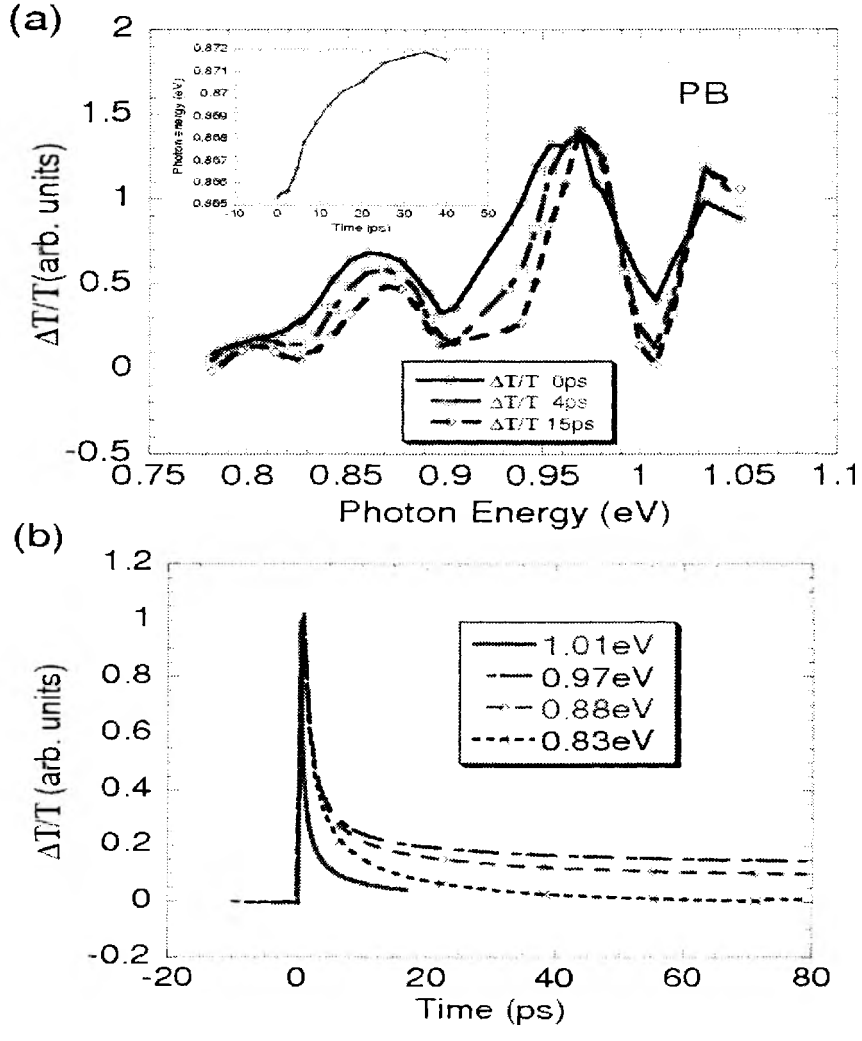

Figure 5: (a) Transient PB spectra of NTs in D_2O solution at three different time delays between the pump and probe pulses; the inset shows the peak position of the PB band at ~ 0.85 eV at various times up to 40 ps. (b) The calculated transient decay of the PB band at various probe photon energies using the model described in the text.

maximum shifts with time by 7 meV in going from t = 0 to t = 35 ps; a similar spectral shift was extracted from the second PB peak at 0.97 eV.

Such spectral diffusion does not occur in the PA bands (Fig. 4(b)), where a uniform time constant of about 3 ps can be inferred. In addition we also found that the PA decay is not exponential; rather, it is a power law in time of the form $(t/t_0)^{-\alpha}$, where $\alpha \approx 0.75$. The power law decay may originate either from dipressive transport type process [41-44], where the exciton diffusion constant towards recombination centers is time dependent [28]; or is due to a distribution of lifetimes, $g(\tau)$ having a tail towards longer time constants of the form $\tau^{-(1+\alpha)}$ and $\alpha \approx 0.75$ [45].

For analyzing the composite PB decay, we assume that there are two transient responses that occur simultaneously. One is a recombination process that has power law decay similar to the PA decay analyzed above, which can be described by the function $t^{-\alpha}$ with $\alpha = 0.75$. The other transient process is a spectral diffusion, where the PB bands blue-shift with time. The transient response across the PB spectrum can be therefore described by the following equation:

$$PB_i(t) = C_{1,i}t^{-\alpha} + C_{2,i}[f_i(t) - f_i(0)], \qquad (1)$$

where PB_i is the response of each of the three sub-bands seen in the transient PB spectrum with index (i); $C_{1,i}$ and $C_{2,i}$ are constants, which are different for each sub-band (i); $\alpha = 0.75$ is the exponent describing the dipressive recombination of both PA and PB responses; $f_i(t)$ describes the transient spectral shift (diffusion) of sub-band (i); and $f_i(0)$ is $f_i(t)$ at t = 0. In Eq. (1) we describe $f_i(t)$ by the relation $f_i(t) = \exp\{-[E-E_{c,i}(t)]^2/2(\delta E)^2\}$, which is a Gaussian function centered at $E_{c,i}(t)$ having a width (δE); and E is the photon energy. At t = 0 we obtained from the transient spectrum of the second PB sub-band at 0.96 eV (namely i = 2 in Eq. (1)) δE = 35 meV; for convenience we assume δE to be time independent and the same for all three measured PB sub-bands. In our model we describe $E_c(t)$ shift with time by the equation:

$$E_{c,i}(t) = E_{c,i}(0) + E_{d,i}[1 - \exp(-t/t_0)], \qquad (2)$$

where $E_{d,i}$ and t_0 are fitting parameters describing the average transient energy shift for the three PB sub-bands. The transient PB dynamics for all wavelengths were fit using Eqs. (1) and (2). We first let the peak maximum for all sub-bands to shift exponentially with time with t_0 = 13 ps (Eq. (2)) that we obtained from the transient spectral shift in Fig. 5(a); whereas $E_{d,i}$ were left as fitting parameters. Also the relative contribution of the two transient contributions to each PB sub-band (namely the decay due to recombination and the spectral shift, which is given by the parameter $C_i = C_{2,i}/C_{1,i}$) were left as fitting parameters. The calculated decay curves for different photon energies using Eqs. (1) and (2) are shown in Fig. 5(b); they are in very good agreement with the experimental data shown in Fig. 4(a). Since the PB decay was fit with the same functional dependence as the PA decay, the agreement between the model calculation and experiment show that the PA and PB share a common underlying mechanism, and are in fact part of the same photoexcitation dynamics process [31].

A surprising finding for the photogenerated excitons in NTs is the existence of transient photoinduced polarization memory (Fig.3, and Fig.6(a)), where $\Delta T_{\parallel} \neq \Delta T_{\perp}$. Fig. 6(a) shows the polarization memory decay, P(t) for isolated NTs in solution. The existence of polarization memory indicates that excitons in 1D *S*-NTs are localized along the NT. This probably is the result of their relatively large binding energy, which makes them close to Frenkel type rather than Wannier type excitons. A number of theoretical models for excitons in *S*-NTs have been recently developed [15-23]. These models put an upper limit for the exciton length at few nanometers, and also showed that the excitons are mainly polarized along the NT direction. Our experimental results are in agreement with these models.

The polarization memory of photogenerated excitons in NTs is not completely lost within the exciton lifetime. The exciton recombination time τ is about 8 ps with a long tail towards longer times (ω_{probe} = 0.96 eV, Fig. 6(a)); whereas the polarization memory hardly decays up to 60 ps (inset of Fig. 6(a)). It is therefore not surprising that we measured polarized PL emission from NTs in solution (Fig. 6(b)), since PL emission originates from the decaying excitons. It is apparent that $PL_{\parallel}$, with polarization parallel to that of the excitation pump, is stronger than the perpendicular component, $PL_{\perp}$; this is true for all measured wavelengths (Fig. 6(b)). We define the PL polarization degree, P_{PL} of the cw emission, as: $P_{PL} = (PL_{\parallel} - PL_{\perp})/(PL_{\parallel} + PL_{\perp})$. From the two measured PL components, we calculated the P_{PL} spectrum (Fig. 6(b)). P_{PL} remains approximately constant at $P^* = 0.14$ ($\pm$ .03) throughout the measured spectrum.

From the average cw PL polarization degree P* it might be possible to calculate the PL lifetime for NTs in solution. Given that the exciton polarization memory decays with time, and can be extrapolated to reach P* = 0.14 at about t = 500 ps (see Fig. 6 (a) inset), we may estimate the average emission time τ_{PL} from the measured P*. From P(t) decay we obtain $\tau_{PL} \approx 500 \pm 100$ ps for NTs in D_2O solution. Our estimated τ_{PL} is not in disagreement with a more direct measurement of transient PL decay [14]. Using the technique of optical Kerr gating, it was measured that PL mostly decays within the first 10 ps, with a very long tail towards longer times. The long tail could not be precisely measured, however, since the optical Kerr gating has a small dynamics range of ~ one order of magnitude for NTs in solution [14]. We note that the obtained τ_{PL} cannot be far off, since otherwise the PL polarization value would have been dramatically different.

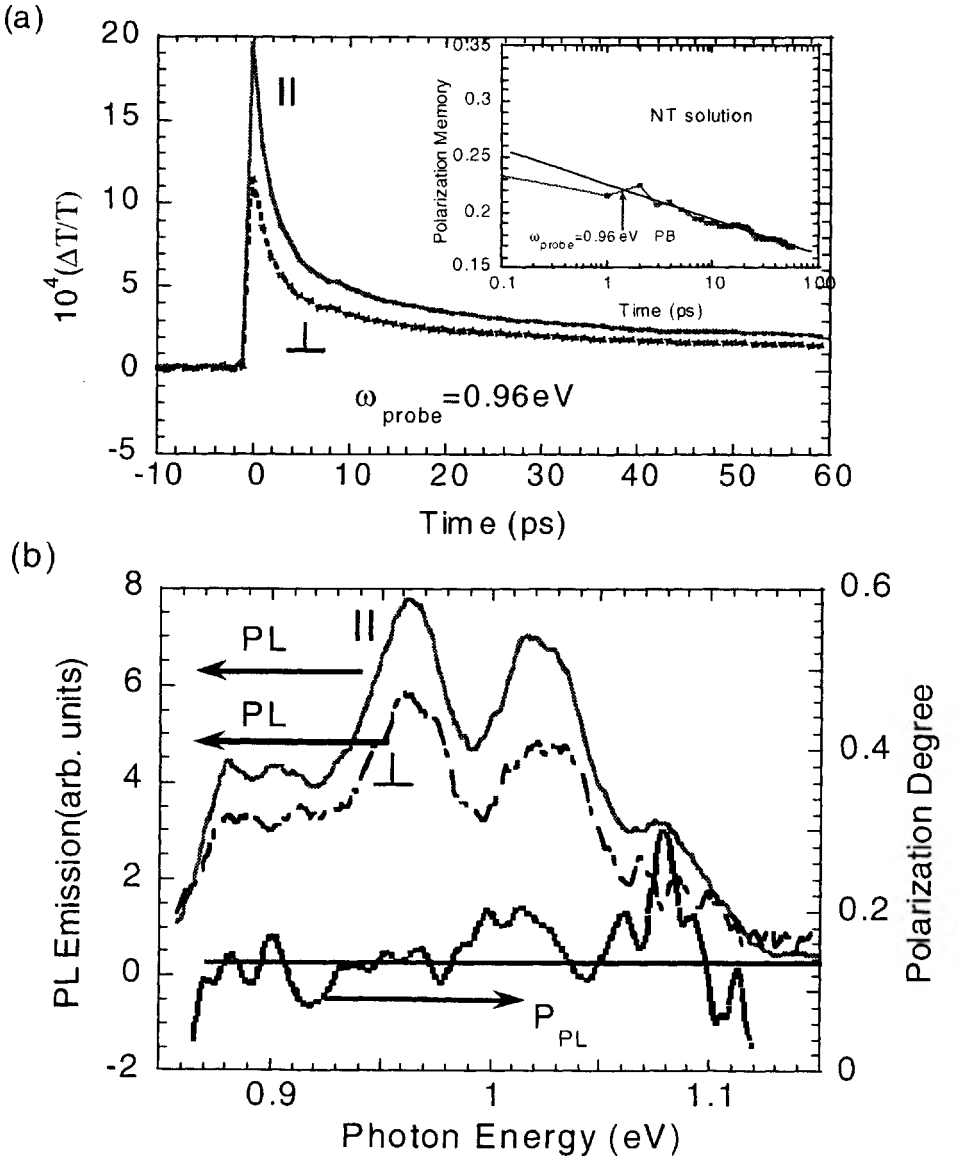

Figure 6: (a) Transient polarized PM response of NTs in D_2O solution at 0.96eV, where both $\Delta T_{\parallel}$ and $\Delta T_{\perp}$ vs. t are shown. The inset is the obtained polarization memory decay, P(t). (b) The parallel and perpendicular components (respect to the pump polarization) of the polarized PL emission spectrum of NTs in solution. The spectrum of the PL polarization degree, P_{PL} (see text) is also shown.

The PL emission band is very weak with estimated quantum efficiency, η of less than 10^{-3} [8, 9]. The most careful estimate of η was made in ref. 14; η was estimated to be 1.7×10^{-4}. In general η is given by the relation [40]:

$$\eta = \tau_{nr}/\tau_r, \qquad (3)$$

where τ_{nr} is the non-radiative recombination lifetime, and τ_r is the radiative recombination lifetime. Some non-radiative recombination channels in organic semiconductors include excitons recombination through deep traps, intersystem crossing to the triplet manifold, and excitons dissociation into polarons [37, 46]. The PL lifetime, τ_{PL} is given in this simple model by the relation [40]:

$$1/\tau_{PL} = 1/\tau_{nr} + 1/\tau_r \qquad (4)$$

Using Eqs. (3) and (4) and the values of τ_{PL} and η from above, we calculate $\tau_{nr} = 500$ ps; whereas τ_r is estimated to be about 3 μsec (with an estimated uncertainty of 2 μsec). This relatively long radiative lifetime indicates that excitons in NTs are basically non-radiative; in other words, their radiative transitions are almost dipole forbidden [23]. This important conclusion should be taken into account in any electron energy calculation in NTs; this is especially true for models in which electron-hole interaction is explicitly included in the calculations [20-23].

4. Conclusions

The present work reemphasizes that the primary photoexcitations in *S*-NT are excitons, rather than free carriers in continuum bands. This conclusion is based on: (i) the photomodulation spectrum, where the PA and PB bands are correlated to each other; (ii) the existence of polarization memory and its decay; and (iii) the similarity between the PL emission, absorption and PB spectra of NTs in D_2O solution.

We studied the ultrafast exciton recombination and polarization memory dynamics in single-walled NTs of different forms, such as annealed and unannealed films and isolated NTs in D_2O solution. We found that the exciton response kinetics depends on the NT environment. When the NT are relatively free of surfactant and defects, then the induced disorder is small and the exciton dynamics are fast, with lifetime of the order of 1 ps. The exciton response dynamics in unannealed films and NTs in D_2O solution are much slower, and this is probably caused by shallow traps in the gap that are introduced by structural defects and impurities on the NT surface; these traps slow down the exciton kinetics. The shallow traps are manifested by: (i) slower exciton diffusion towards recombination centers, which reduces the recombination rate; and (ii) a slower rate for the exciton polarization memory decay.

We also measured polarized PL emission in NTs in D_2O solution with bands that follow the absorption sub-bands. We found that the average PL polarization degree P* remains constant at 0.14 across the PL spectrum. From the value of P* and the exciton polarization memory decay dynamics for NT in solution we estimated the PL lifetime in NT to be about 500 ps. From this relatively long PL lifetime, coupled with the tiny PL emission quantum efficiency, we estimate the radiative transition time in NT to be of the order of 3±2 μsec.

5. Acknowledgements

This work was supported in part by the NSF (DMR 02-02790) and a grant in aid from the University of Utah. At the University of Texas at Dallas, the work was supported by DARPA grant No. MDA 972-02-C-005 and the Robert A. Welch foundation.

References

1. A. B. Dalton, S. Collins, E. Munoz, J.M. Razal, V.H. Ebron, J.P. Ferraris, J.N. Coleman, B.G. Kim, and R.H. Baughman, Nature **423**, 703 (2003).
2. P. G. Collins, A. Zettl, H. Bando, A. Thess, R.E. Smalley, Science **278,** 100 (1997).
3. R. Saito, G. Dresselhaus, and M. S. Dresselhaus, *Physical Properties of Carbon Nanotubes* (Imperial College Press, London, 1999).
4. Z. M. Li, Z.K. Tang, H.J. Liu, N. Wang, C.T. Chan, R. Saito, S. Okada, G.D. Li, J.S. Chen, N. Nagasawa, and S. Tsuda, Phys. Rev. Lett. **87,** 127401 (2001).
5. W. Z. Liang, G.H. Chen, Z.M. Li, Z.K. Tang, Appl. Phys. Lett. **80**, 3415 (2002).
6. G.S. Duesberg, I. Loa, M. Burghard, K. Syasssen, and S. Roth, Phys. Rev. Lett. **85,** 5436 (2000).
7. A. Hartschuh, H. N. Pedrosa, L. Novotny, and T. D. Krauss, Science **301**, 1354 (2003).
8. M.J. O'Connell, S.M. Bachilo, C.B. Huffman, V.C. Moore, M.S. Strana, E.H. Haroz, K.L. Rialon, P.J. Boul, W.H. Noon, C. Kittrell, J.P. Ma, R.H. Hauge, R.B. Weisman, R.E. Smalley, Science **297**, 593 (2002).
9. S. M. Bachilo, M. S. Strano, C. Kittrell, R. H. Hauge, R. E. Smalley, and R. B. Wiesman, Science **298**, 2361 (2002).
10. J. Lefebvre, Y. Homma, and P. Finnie, Phys. Rev. Lett. **90,** 217401 (2003).
11. J. A. Misewich, R. Martel, Ph. Avouris, J. C. Tsang, S. Heinze, and J. Tersoff, Science **300**, 783 (2003).
12. M. Freitag, J. Chen, J. Tersoff, J. C. Tsang, Q. Fu, J. Liu, and Ph. Avouris, Phys. Rev. Lett. **93**, 076803 (2004).
13. J. Lefebvre, J. M. Fraser, P. Finnie, and Y. Homma, Phys. Rev. B **69**, 075403 (2004).
14. F. Wang, G. Dukovic, L. E. Brus, and T. F. Heinz, Phys. Rev. Lett. **92**, 177401 (2004).
15. T. Ando, Jour. Phys. Soc. Japan **66**, 1066 (1997).
16. M. Ichida, S. Mizuno, Y. Tani, Y. Saito, and A. Nakamura, Jour. Phys. Soc. Japan **68,** 3131 (1999).
17. C. L. Kane and E.J. Mele, Phys. Rev. Lett. **90,** 207401 (2003).
18. T.G. Pedersen, Phys. Rev. **B 67**, 073401 (2003).
19. M. Ichida, S. Mizuno, Y. Saito, H, Kataura, Y. Achiba, and A. Nakamura, Phys. Rev. **B 65**, 241407 (2002).
20. C. D. Spataru, S. Ismail-Beigi, L. X. Benetict, and S. G. Louie, Phys. Rev. Lett, **92**, 077402 (2004).
21. E. Chang, G. Bussi, A. Ruini, amd E. Molinari, Phys. Rev. Lett. **92**, 196401 (2004).
22. V. Perebeinos, J. Tersoff, and Ph. Avouris, Phys. Rev. Lett. **92**, 257402 (2004).
23. H. Zhao and S. Mazumdar, Phys. Rev. Lett. (in press); Cond-mat/0406203.
24. M. Chandross and S. Mazumdar, Phys. Rev. B **55**, 1497 (1997).
25. M. J. Rice and Y. N. Gartstein, Phys. Rev. Lett. **73**, 2504 (1994).
26. A. Race, W. Barford,, and R. J. Bursill, Phys. Rev. B **64**, 035208 (2001).
27. T. Hertel and G. Moos, Chem. Phys. Lett, **320**, 359 (2000); Phys. Rev. Lett. **84**, 5002 (2000).
28. Y.C. Chen, N.R. Raravikar, L.S. Schadler, P.M. Ajayan, Y.P. Zhao, T.M. Lu, G.C. Wang, and X.C. Zhang, Appl. Phys. Lett. **81**, 975 (2002).
29. S. Tatsuura, M. Furuki, Y. Sato, I. Iwasa, M. Tian, and H, Mitsu, Adv. Mater. **15**, 534 (2003).
30. J. S. Lauret, C. Voisin, G. Cassabois, C. Delalande, Ph. Roussignol, O. Jost, and L. Capes, Phys. Rev. Lett, **90**, 057404 (2003).
31. O. J. Korovyanko, C. -X. Sheng, Z.V. Vardeny, A.B. Dalton, and R.H. Baughman, Phys. Rev. Lett **92**, 017403 (2004).
32. G. N. Ostojic, S. Zaric, J. Kono, M. S. Strano, V. C. Moore, R. H. Hauge, and R. E. Smalley, Phys. Rev. Lett. **92**, 117402 (2004).
33. P. Nikolaev, M. J. Bronikowski, K. Bradley, F. Rohmund, D.T. Colbert, K.A. Smith, and R.E. Smalley, Chem. Phys. Lett. **313**, 91 (1999).
34. G.U. Sumanasekera, C.K.W. Adu, S. Fang, and P.C. Eklund, Phys. Rev. Lett. **85**, 1096 (2000).
35. M.E. Itkis, S. Niyogi, M.E. Meng, M.A. Hamon, H. Hu and R.C. Haddon, Nano Lett. **2**, 155 (2002).
36. T. Pichler, M. Knupfer, M. S. Golden, J. Fink, A. Rinzler, and R. E. Smalley, Phys. Rev. Lett. **80**, 4729 (1998).
37. S.V. Frolov, M. Liess, P. A. Lane, W. Gellermann, and Z.V. Vardeny, Phys. Rev. Lett. **78**, 4285 (1997).
38. P. M. Rafilov, H. Jantoljak, and C. Thomsen, Phys. Rev. B **61**, 16179 (2000).
39. M. Hulman, W. Plank, and H. Kuzmany, Phys. Rev. B **63**, R081406 (2001).
40. J. Pankove, *Optical processes in semiconductors* (Englewood Cliffs, N.J., Prentice-Hall 1971).
41. Z. Vardeny and J. Tauc, *Semiconductors Probed by Ultrafast Laser spectroscopy*, edited by R. R. alfano (Academic, Orlando, FL, 1984), Vol 2, p. 23.

42. Z. Vardeny, J. Strait, and J. Tauc, Appl. Phys. Lett. **42**, 580 (1983).
43. R. A. Cheville and N. J. Halas, Phys. Rev. B **45**, R4548 (1992).
44. Z. Vardeny, P. O'Connor, S. Ray and J. Tauc, Phys. Rev. Lett. **44**, 1267 (1980).
45. Z. Vardeny, J. Strait, D. Pfost, J. Tauc and B. Abeles, Phys. Rev. Lett. **48**, 1132-1136 (1982).
46. M. Wohlgenannt, W. Graupner, G. Leising and Z. V. Vardeny, Phys. Rev. B **60**, 5321-5330 (1999).